Front. Optoelectron. China 2011, 4(2): 195–198
DOI 10.1007/s12200-011-0164-7

RESEARCH ARTICLE

Bis-(8-hydroxyquinoline) copper nanoribbons: preparation, characterization, and photoconductivity

Qi SHAO[1,2], Tao WANG[1], Xiuhua WANG[2,3], Youcun CHEN (✉)[1]

1 Anhui Key Laboratory of Functional Coordination Compounds, School of Chemistry and Chemical Engineering,
Anqing Normal University, Anqing 246011, China
2 Institute of Functional Nano & Soft Materials (FUNSOM) and Jiangsu Key Laboratory for Carbon-Based Functional Materials & Devices,
Soochow University, Suzhou 215123, China
3 Anhui Key Laboratory of Functional Molecular Solids, College of Chemistry and Materials Science, Anhui Normal University,
Wuhu 241000, China

Abstract Bis-(8-hydroxyquinoline) copper nanoribbons with an average width of 400 nm, a thickness of 70 nm and the length of up to tens of micrometers, were synthesized by a facile solvothermal method. X-ray powder diffraction and Fourier transform infrared spectrum were employed to determine their structure. The photoconductivity of a bundle of nanoribbons was also measured, which exhibited unique photoresponse to light, indicating their potential applications in photoswitch nanodevices in the future.

Keywords 8-hydroxyquinoline, nanoribbons, photoswitches

1 Introduction

In the past decades, one-dimensional (1D) nanostructures have aroused tremendous development thanks to their unique electronic and optic properties and prospective applications in nanometer-scale devices [1–4]. Nowadays, 1D organic nanomaterials have emerged as promising and prospective next-generation materials due to the noncovalent intermolecular interactions such as hydrogen bonding, Van der Waals force, and π-π stacking [5–9].

Since Tang first reported the efficient low-voltage-driven organic light-emitting diodes based on tris-(8-hydroxyquinoline) aluminium (AlQ_3) in 1987 [10], 8-hydroxyquinoline complexes have attracted wide attentions as important organic semiconductors materials because of their excellent electronic and optical properties, and broad applications in many fields [11–14]. Recently, Li et al. synthesized bis-(8-hydroxyquimoline) cadmium (CdQ_2) nanorods via a solution based route with surfactant [15]. Zhu et al. obtained bis-(8-hydroxyquinoline) zinc (ZnQ_2) by sonochemical route from the water/oil microemulsion [16]. Wang et al. synthesized ZnQ_2 by solvothermal method [17].

In this work, a facile solvothermal method without the assistance of templates and the contamination from the surfactants was employed to prepare bis-(8-hydroxyquinoline) copper (CuQ_2) nanoribbons. A photoconduction device was fabricated based on the nanoribbons and the photoconductive property was measured. The products exhibited fast and reversible photoswitching response under on/off light exposure conditions.

2 Experiment

2.1 Materials

All the chemical regents were of analytical grade and used without further purification.

2.2 Preparation of CuQ_2 nanoribbons

In a typical synthesis, 0.5 mmol $CuCl_2$ and 1 mmol 8-hydroxyquinoline were dissolved into 40 mL methanol under stirring, which was transferred into a Teflon-lined autoclave of 60 mL capacity and heated to 140°C for 10 h and cooled to room temperature naturally. Then ultrapure water was added into the resulting solution dropwise under violent stirring. The resulting suspension was separated centrifugally, washed with ultrapure water for several times, and then dried under vacuum at 60°C for 12 h.

Received November 15, 2010; accepted November 30, 2010

E-mail: chenyc@aqtc.edu.cn

2.3 Characterization

The powder X-ray diffraction (XRD) pattern was recorded on a Shimadzu XRD-6000 X-ray diffractometer equipped with Cu Kα radiation ($\lambda = 0.15406$ nm); a scanning rate of 0.05°/s was applied to record the pattern in the 2θ range of 5°–50°. The morphology and size of the products were studied by a Hitachi S-4800 scanning electron microscope (SEM). Fourier transform infrared (FTIR) spectrum was obtained with KBr pellets for solids on a Shimadzu FTIR-8400S spectrometer. The electrical measurements were tracked with a CHI 620B electrochemical workstation. The low magnification image was taken from an Olympus optical microscope.

3 Results and discussion

The XRD pattern of the as-prepared CuQ_2 nanoribbons is shown in Fig. 1. The peaks at $2\theta = 8.18°$, 16.44°, 24.78°, 33.22°, and 41.90° are strong. The elemental analysis (EA) is carried out with a Heraeus CHN-O Rapid instrument. The EA results of the sample show that the contents of C, N, and H are 62.55%, 8.02%, and 3.31%, respectively. The values are consistent with the calculated values (C: 61.46%; N: 7.96%; H: 3.41%) of CuQ_2.

The FTIR spectrum is recorded to reveal the composition of CuQ_2, as shown in Fig. 2. The quinoline's characteristic stretching vibrations (1763–1458 cm^{-1}, 1384 cm^{-1}, 814 cm^{-1}, 671 cm^{-1}), aromatic amine resonances (C-N, 1384 cm^{-1}) and the C-O stretching vibration at 1045 cm^{-1} are clearly observed. The peaks at 505 and 428 cm^{-1} are assigned to the Cu-O and Cu-N stretching vibration respectively. All of the vibrations may be assigned to CuQ_2 [18,19], which further supports that the as-prepared products are pure CuQ_2.

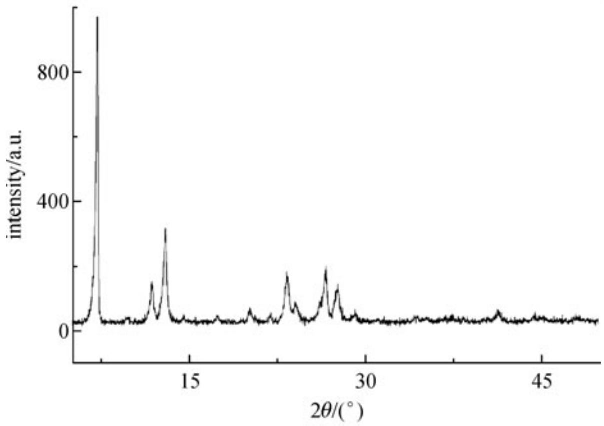

Fig. 1 XRD pattern of products

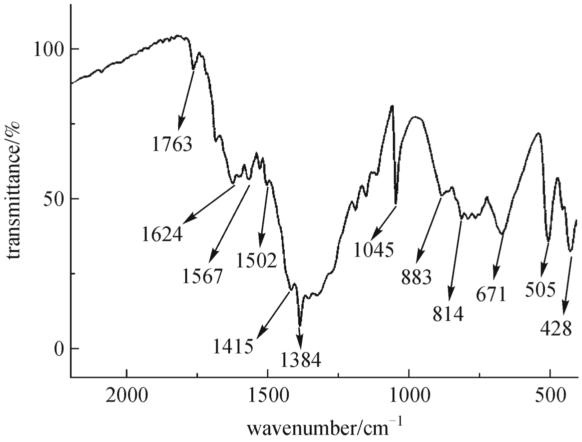

Fig. 2 FTIR spectrum of products

Figure 3(a) displays a panoramic SEM image of the as-prepared CuQ_2, which shows the ribbon-like morphology with lengths up to tens of micrometers. The high magnification SEM image shown in Fig. 3(b) further

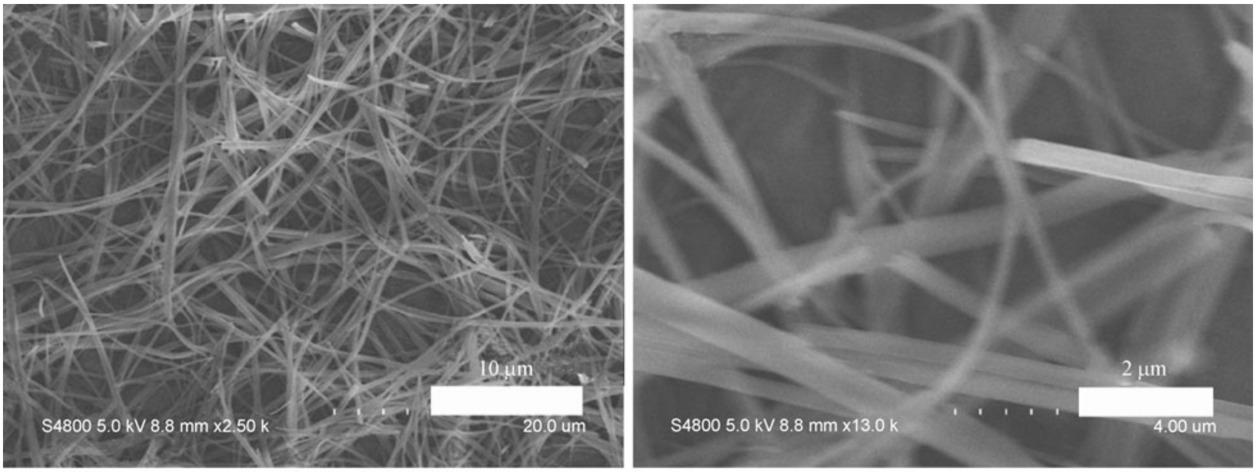

(a) (b)

Fig. 3 SEM images of products. (a) Low magnification; (b) high magnification reveals the ribbons with an average width of 400 nm and a thickness of 70 nm.

To measure the conductivity of the products, indium tin oxide (ITO) coated glass with the electrode gap of 25 μm was employed as the substrate. A bundle of CuQ_2 nanoribbons were dispersed and bridged over the electrodes with an effective length of about 35 μm, as shown in the inset of Fig. 4. To increase injection of the device, gold gap electrodes were fabricated on the substrate by thermal evaporation with a micrometer-sized Au wire as the mask; with a slight movement of the Au-wire mask, Au-Au gap electrodes were deposited [20]. Then the conductivity was measured in a dark box or under illumination with an incandescence lamp (12 V, 10 W). In order to decrease thermal effect, the power of the incandescence lamp was only 10 W and the distance of the device-to-light source was 10 cm.

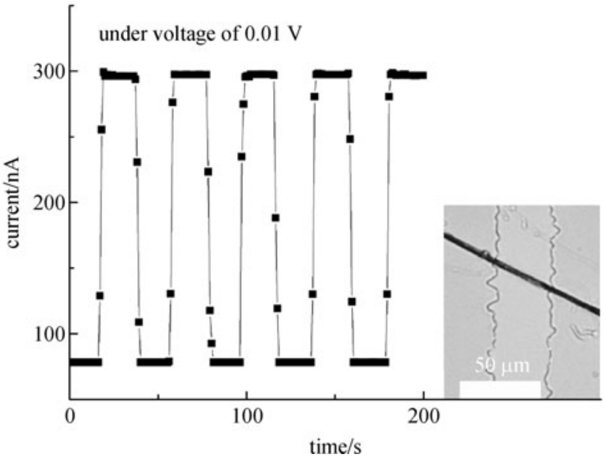

Fig. 4 Photoresponse characteristics of a bundle of products during light switching on/off, and image of a bundle of products between two Au electrodes from optical microscope (inset)

Figure 4 shows the photoresponse characteristic of CuQ_2 with light switched on/off. A voltage of 0.01 V was applied across the two electrodes and the current recorded during the light was alternatively on and off at 20 s intervals. It is clearly observed that the conductivity of the CuQ_2 nanoribbons promptly increases or decreases with the illumination on/off, which shows that the products have an excellent photoresponse. Under illumination, the energy from the light excites the electrons in the semiconductor CuQ_2 jumping from the valence band into the conduction band, leaving holes in valence band and increasing the charge carrier concentration via direct electron-hole pair creation, and thus enhancing the current of the nanoribbons [21].

4 Conclusion

In summary, large-scale CuQ_2 nanoribbons were successfully synthesized via a facile solvothermal approach without use of template or surfactant. The photocurrent of a bundle of CuQ_2 exhibited unique, fast and reversible photoswitching response. This work might have potential application in organic semiconductive or photosensitive nanodevices in the future.

Acknowledgements This work was supported by the National Natural Science Foundation of China (Grant No. 20571001), and the Anhui Provincial Natural Science Foundation of Universities (No. KJ2009B003Z).

References

1. Zhang X J, Zhang X H, Zou K, Lee C S, Lee S T. Single-crystal nanoribbons, nanotubes, and nanowires from intramolecular charge-transfer organic molecules. Journal of the American Chemical Society, 2007, 129(12): 3527–3532
2. An B K, Lee D S, Lee J S, Park Y S, Song H S, Park S Y. Strongly fluorescent organogel system comprising fibrillar self-assembly of a trifluoromethyl-based cyanostilbene derivative. Journal of the American Chemical Society, 2004, 126(33): 10232–10233
3. Zhao L Y, Yang W S, Luo Y, Zhai T Y, Zhang G J, Yao J N. Nanotubes from isomeric dibenzoylmethane molecules. Chemistry, 2005, 11(12): 3773–3778
4. Xia Y N, Yang P D, Sun Y G, Wu Y Y, Mayers B, Gates B, Yin Y D, Kim F, Yan H Q. One-dimensional nanostructures: synthesis, characterization, and applications. Advanced Materials, 2003, 15 (5): 353–389
5. Zhang X J, Jie J S, Zhang W F, Zhang C Y, Luo L B, He Z B, Zhang X H, Zhang W J, Lee C S, Lee S T. Photoconductivity of a single small-molecule organic nanowire. Advanced Materials, 2008, 20 (12): 2427–2432
6. Hu J S, Guo Y G, Liang H P, Wan L J, Jiang L. Three-dimensional self-organization of supramolecular self-assembled porphyrin hollow hexagonal nanoprisms. Journal of the American Chemical Society, 2005, 127(48): 17090–17095
7. Zhao Y S, Fu H B, Peng A D, Ma Y, Xiao D B, Yao J N. Low-dimensional nanomaterials based on small organic molecules: preparation and optoelectronic properties. Advanced Materials, 2008, 20(15): 2859–2876
8. Chiu J J, Kei C C, Perng T P, Wang W S. Organic semiconductor nanowires for field emission. Advanced Materials, 2003, 15(16): 1361–1364
9. Liu H B, Zhao Q, Li Y L, Liu Y, Lu F S, Zhuang J P, Wang S, Jiang L, Zhu D B, Yu D P, Chi L F. Field emission properties of large-area nanowires of organic charge-transfer complexes. Journal of the American Chemical Society, 2005, 127(4): 1120–1121
10. Tang C W, VanSlyke S A. Organic electroluminescent diodes. Applied Physics Letters, 1987, 51(12): 913–915
11. Chiu J J, Wang W S, Kei C C, Perng T P. Tris-(8-hydroxyquinoline) aluminum nanoparticles prepared by vapor condensation. Applied Physics Letters, 2003, 83(2): 347–349
12. Hu J S, Ji H X, Cao A M, Huang Z X, Zhang Y, Wan L J, Xia A D, Yu D P, Meng X M, Lee S T. Facile solution synthesis of hexagonal

AlQ$_3$ nanorods and their field emission properties. Chemical Communications, 2007, (29): 3083–3085

13. Wang X H, Shao M W, Shao G, Wang S W. Tris(8-hydroxyquinoline) aluminum nanoribbons: facile solvothermal preparation and photoconductivity studies. Journal of Nanoscience and Nanotechnology, 2009, 9(8): 4709–4714
14. Cho C P, Yu C Y, Perng T P. Growth of AlQ$_3$ nanowires directly from amorphous thin film and nanoparticles. Nanotechnology, 2006, 17(21): 5506–5510
15. Chen W, Peng Q, Li Y D. Luminescent bis-(8-hydroxyquinoline) cadmium complex nanorods. Crystal Growth & Design, 2008, 8(2): 564–567
16. Pan H C, Liang F P, Mao C J, Zhu J J, Chen H Y. Highly luminescent zinc(II)-bis(8-hydroxyquinoline) complex nanorods: sonochemical synthesis, characterizations, and protein sensing. The Journal of Physical Chemistry B, 2007, 111(20): 5767–5772
17. Wang X H, Shao M W, Liu L. High photoluminescence and photoswitch of bis(8-hydroxyquinoline) zinc nanoribbons. Synthetic Metals, 2010, 160(7–8): 718–721
18. Fanning J C, Jonassen H B. The reaction of 8-quinolinol with copper (II) salts. Journal of Inorganic and Nuclear Chemistry, 1963, 25(1): 29–35
19. Tackett J E, Sawyer D T. Properties and infrared spectra in the potassium bromide region of 8-quinolinol and its metal chelates. Inorganic Chemistry, 1964, 3(5): 692–696
20. Tang Q X, Li H X, Liu Y L, Hu W P. High-performance air-stable n-type transistors with an asymmetrical device configuration based on organic single-crystalline submicrometer/nanometer ribbons. Journal of the American Chemical Society, 2006, 128(45): 14634–14639
21. Li Q H, Wan Q, Liang Y X, Wang T H. Electronic transport through individual ZnO nanowires. Applied Physics Letters, 2004, 84(22): 4556–4558